Geochemistry, Geophysics, Geosystems®

AGU ADVANCING EARTH AND SPACE SCIENCE

RESEARCH ARTICLE
10.1029/2022GC010536

Phosphorus Variations in Volcanic Sequences Reveal the Linkage Between Regional Tectonics and Terrestrial Biota Evolution

Chao Ma[1,2], Yanjie Tang[1,2], Stephen F. Foley[3,4], Chenyang Ye[1,2], Jifeng Ying[1,2], Xinmiao Zhao[1], Yan Xiao[1], and Hongfu Zhang[1,2]

[1]State Key Laboratory of Lithospheric Evolution, Institute of Geology and Geophysics, Chinese Academy of Sciences, Beijing, China, [2]College of Earth and Planetary Sciences, University of Chinese Academy of Sciences, Beijing, China, [3]School of Natural Sciences, Macquarie University, North Ryde, NSW, Australia, [4]Research School of Earth Sciences, Australian National University, Canberra, ACT, Australia

Key Points:

- The paleo-Pacific subduction triggered the cratonic destruction and thus controlled the intensity of volcanism in the Middle–Late Mesozoic
- The change of lithospheric thickness triggered by the paleo-Pacific subduction caused the variation of P content in the volcanics
- Regional tectonics could impact the evolution of terrestrial ecosystems through the volcanism and nutrient P cycle

Supporting Information:

Supporting Information may be found in the online version of this article.

Correspondence to:

Y. Tang,
tangyanjie@mail.iggcas.ac.cn

Citation:

Ma, C., Tang, Y., Foley, S. F., Ye, C., Ying, J., Zhao, X., et al. (2022). Phosphorus variations in volcanic sequences reveal the linkage between regional tectonics and terrestrial biota evolution. *Geochemistry, Geophysics, Geosystems*, *23*, e2022GC010536. https://doi.org/10.1029/2022GC010536

Received 24 MAY 2022
Accepted 20 JUL 2022

Abstract The Middle–Late Mesozoic massive volcanism formed a considerable thickness of volcanic-sedimentary strata in western Liaoning, northern China. Concomitantly, it elevated phosphorus (P) availability for the rapid bloom of the terrestrial Yanliao and Jehol biotas, which developed highly abundant biodiversity and biomass. Hence, systematic tectonic and geochemical analyses of these volcanic-sedimentary sequences with a significant P fluctuation would advance our understanding of the coevolutionary relationship between terrestrial biotas and regional tectonics. Here, we show that the secular variation of P availability in the Mesozoic volcanic rocks were the immediate results of the changes in volcanic intensity and lithospheric thickness controlled by the geological background of the cratonic destruction resulting from the paleo-Pacific plate subduction. This study reveals the constraint effect of regional tectonics on the evolution of terrestrial ecosystems through the volcanism and P cycle.

Plain Language Summary The phosphorus (P) is necessary for biotas and mainly comes from volcanics in areas dominated by volcanism closely related to deep-Earth processes. Thus, the origin of P changes in volcanics can provide key evidence for the intrinsic relations between deep processes and biota evolution. Here, we present tectonic and geochemical analyses for the Mesozoic fossil-bearing volcanic-sedimentary strata in northern China. The westward subduction of the paleo-Pacific plate triggered the crustal thickening and subsequent lithospheric thinning of the East Asia continent. These dynamic processes controlled the volcanic intensity and P variation, resulting in remarkable changes in P availability that led to the rise and fall of terrestrial biotas. Hence, P variations in volcanic sequences reveal the linkage between regional tectonics and biota evolution. This study represents an effort to explore how tectonic processes constrained terrestrial biotas involving multidisciplinary methods.

1. Introduction

Tectonism has a crucial influence on biological evolution by altering topography, climate, environment and material supply (McKenzie et al., 2014; Santosh, 2010; Zaffos et al., 2017), such as the supercontinent cycle and Cambrian explosion. Plate tectonics links the biosphere with deep Earth, ensuring a geochemical cycle of nutrients that sustains life (Zerkle, 2018; Zerkle & Mikhail, 2017). Phosphorus (P) is a principal limiting nutrient in the biosphere (Kipp & Stüeken, 2017; Reinhard et al., 2017) and is essential to primary production, decomposition, and other biological processes in diverse terrestrial ecosystems (Du et al., 2020; Porder & Ramachandran, 2012). P has no significant gaseous form, meaning that P can only be obtained from the weathering of bedrock, including rocks and deposits (Hahm et al., 2014; Porder & Ramachandran, 2012; Ruttenberg, 2014). The weathering products with available P, directly transported into the ecosystems, will provide a fundamental limitation on the expansion and evolution of terrestrial biotas, especially the bloom of terrestrial floras (Hartmann et al., 2014; Ott, 2020). Fresh volcanic rocks, one of the most critical P reservoirs (Porder & Ramachandran, 2012), contain higher P contents than the crustal mean and typical sediments (Rudnick & Gao, 2014). They can more effectively transfer available P to the biosphere due to extensive exposed areas after eruptions (Lee et al., 2018). Hence, volcanism with different P availability is a crucial link between the deep Earth and the biosphere.

The notable Yanliao and Jehol biotas, with abundant well-preserved fossils and biodiversity in northern China especially western Liaoning (Figure 1), open a window into the Middle–Late Mesozoic terrestrial ecosystems (Zhou et al., 2021; Zhou & Wang, 2017). The bloom of the two terrestrial biotas appeared spatiotemporally related to the initial and peak stages of the destruction of the North China craton (NCC) in the Middle Jurassic and the Early Cretaceous, respectively (Zhou et al., 2021; Zhu et al., 2020). Nevertheless, how the cratonic destruction impacted the terrestrial Yanliao and Jehol biotas remains largely unknown. The geodynamical and geochemical analyses can conduce to understanding the response process and coupling mechanism between biological evolution and tectonism.

During the Middle–Late Mesozoic, massive volcanism occurred on the NCC, mainly from the Middle–Late Jurassic to the Early Cretaceous (Ma & Xu, 2021; Wu et al., 2019; Zhang et al., 2014). They formed the thick volcanic-sedimentary strata, such as the Haifanggou/Jiulongshan, Lanqi/Tiaojishan, Dabeigou/Huajiying, Yixian, and Jiufotang formations in western Liaoning, northern Hebei, southern Inner Mongolia, and west Shandong (Wu et al., 2019; Zhang et al., 2014). The exposure of the bedrock to subaerial weathering resulted in the gray and brown volcanic rocks and paleosol development in the Sichakou Basin, northern Hebei (Yang et al., 2020). Due to the different volumes between the volcanic deposits and the contemporaneous non-volcanic sediments (Huang, 2019), volcanic P controlled the variation of available P in the terrestrial environment affected by volcanism (Longman et al., 2021; Ma, Tang, & Ying, 2022).

The spatiotemporal distribution of volcanism roughly coincided with the blooms of the Yanliao and Jehol biotas, as evidenced by the explosion of biodiversity preserved in coeval sedimentary stratigraphic sequences (Zhou & Wang, 2010), which suggests that the volcanic rocks determined the upper limit of available P supply for the terrestrial biotas. The spatiotemporal relationship between the *volcanic P availability* (VPA) and biotas suggests that the increased VPA may trigger the emergence and expansion of the Yanliao and Jehol biotas (Figure 2). Hence, volcanic P delivery from the deep Earth to the surface provides a strong material basis for biological evolution. However, the driving mechanism for the variation of the P supply remains unclear, preventing us from understanding the inherent relationship between regional tectonics and terrestrial biotas.

Hence, we select the fossil-bearing volcanic-sedimentary strata (Figure 1d), including the Jurassic Haifanggou–Lanqi formations and the Early Cretaceous Yixian Formation in western Liaoning, northern China, to reveal the linkage between tectono-magmatic activities and terrestrial biotas. By integrating new data with those published Middle–Late Mesozoic volcanic geochemical data from northern China, we will calculate geochemical proxies to elucidate their temporal variations and the impacts of regional tectonics on the terrestrial biota evolution through the P cycle.

2. The Yanliao and Jehol Biotas

Two Mesozoic terrestrial biotas in northern China, the Yanliao and Jehol, unquestionably represent world-class *Lagerstätten* in terms of biodiversity and fossil preservation (Xu et al., 2020; Zhou & Wang, 2010, 2017). The Yanliao Biota preserved many earliest known organisms, including angiosperms, feathered dinosaurs, gliding and aquatic mammaliaforms, and eutherian mammals (Chang et al., 2009; Xu et al., 2016; Zhou & Wang, 2017). It has thus emerged as an indispensable biota for understanding the evolution of many major groups of organisms in the Mesozoic terrestrial environment, including the origins of some large modern clades (Xu et al., 2016). The Jehol Biota is one of the unique Mesozoic terrestrial biotas globally (Xu et al., 2020; Yang et al., 2020). It has significantly advanced our understanding of the origins or early evolution of many organisms, including angiosperms, birds, eutherian and metatherian mammals, and insects (Zhou et al., 2021). Exceptionally, theropod fossils unearthed from the Jehol Biota provide solid and comprehensive evidence for the hypothesis that birds are descendants of dinosaurs (Zhou & Wang, 2017). The Jehol bird assemblage documents the earliest radiation in the origin and evolution of birds (Xu et al., 2020). The Jehol plant fossils cover nearly all major plant groups, especially flowering plants, with crucial evolutionary implications (Dilcher, 2000).

The growing geochronologic data put a tight constraint on the ages of the Yanliao (ca. 165–158 Ma) and Jehol (ca. 135–120 Ma) biotas (Yang et al., 2020; Zhou & Wang, 2017). They shared a similar geographic distribution, mainly located in western Liaoning, northern Hebei, and southeastern Inner Mongolia, belonging to the north margin of the NCC. In contrast, the Jehol Biota seemed to be more widely distributed. They are preserved in the lacustrine sediments (mainly tuffaceous shales or mudstones) and often interbedded with tuffaceous layers (Xu

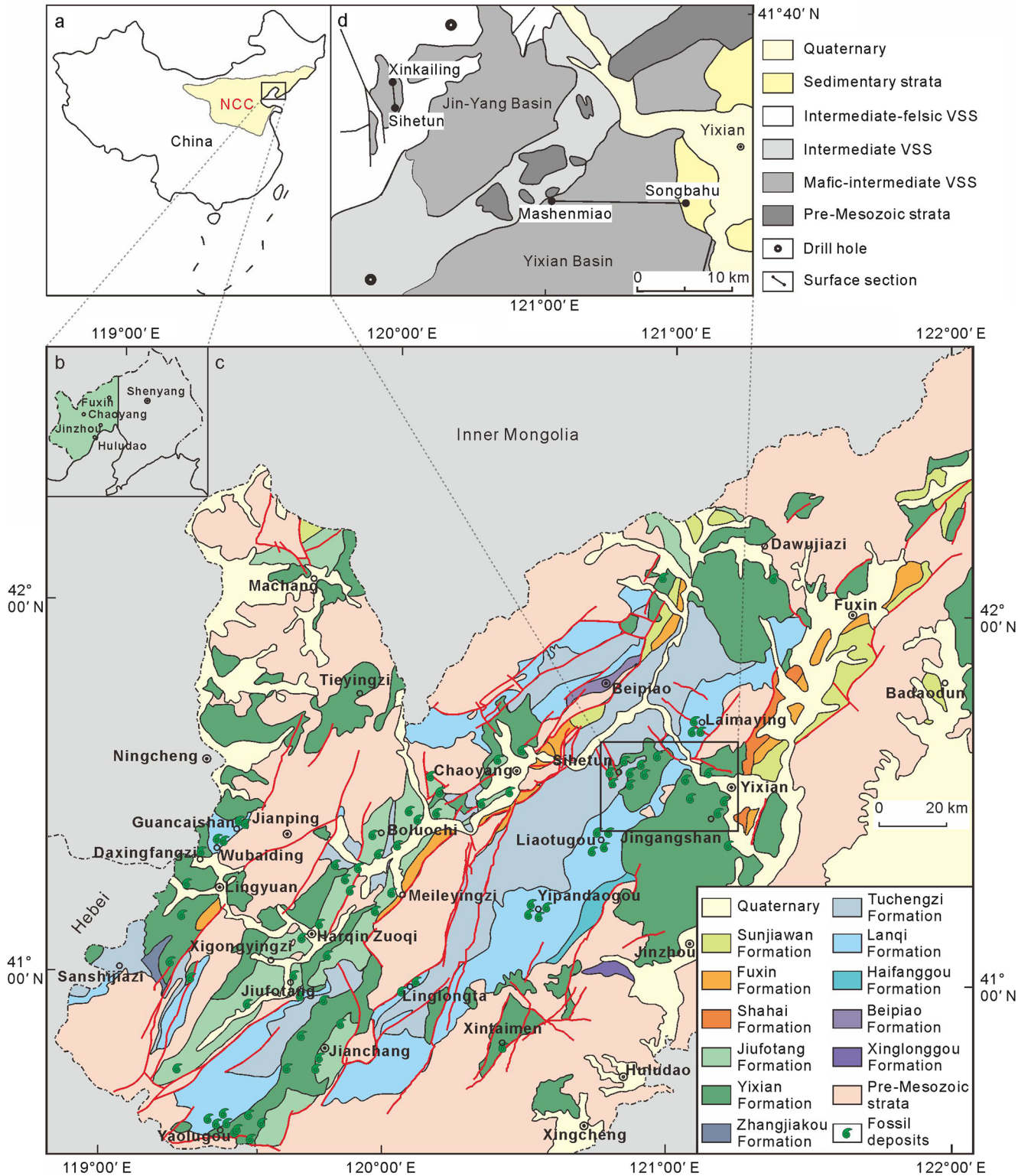

Figure 1. Geological map of western Liaoning (northern North China craton) showing the location of Jurassic drill holes, the Early Cretaceous Xinkailing–Sihetun and Mashenmiao–Songbahu sections, modified from Wang et al. (2006) and Zhang (2013). The drill cores include the volcanic-sedimentary strata of Haifanggou and Lanqi formations. The two sections record volcanic-sedimentary strata of the Yixian Formation.

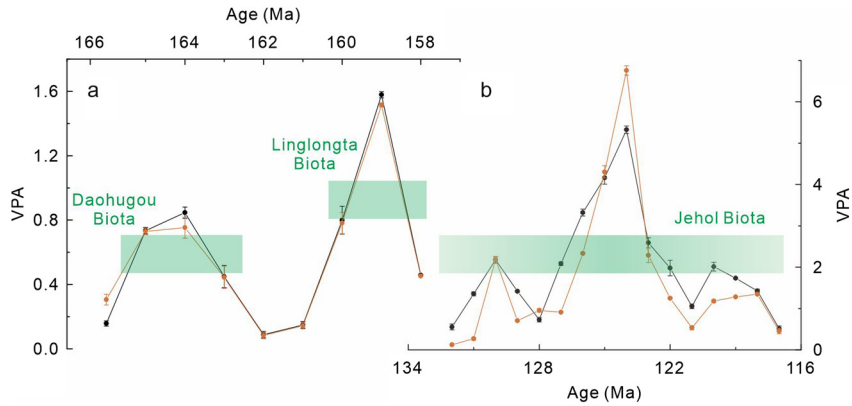

Figure 2. Temporal variation of *volcanic P availability* (VPA) in volcanic rocks and dominant lithology. Data are calculated from the compiled metadata (Supporting Information S1). (a) The black line represents the overall VPA of the Middle–Late Jurassic volcanic rocks, while the red represents the VPA of felsic rocks. (b) The black line represents the overall VPA of the Early Cretaceous volcanic rocks, while the red represents the VPA of mafic rocks. The green labels represent the periods of the Yanliao and Jehol biotas. The Early Cretaceous VPA spike occurred at ca. 124 Ma, approximately corresponding to the most momentous biological radiations of the Jehol Biota. The Jurassic VPA spikes correspond to the two phases of the Yanliao Biota, the Daohugou Biota (ca. 165–163 Ma) and Linglongta Biota (ca. 160–158 Ma).

et al., 2016; Zhou et al., 2021). The typical Yanliao Biota mainly occurred in the Haifanggou/Jiulongshan and Lanqi/Tiaojishan formations (Zhou et al., 2010). The Jehol Biota only emerged in the Huajiying, Yixian, and Jiufotang formations (Pan et al., 2013). Volcanic, pyroclastic, and volcanic-sedimentary rocks are commonplace in these strata (Huang, 2019; Jiang & Sha, 2006).

3. Samples and Methods

3.1. Samples

Some geochemical data of the Middle–Late Mesozoic volcanic rocks on the NCC are from the freely accessible EarthChem (https://earthchem.org/) rock database. The data structure includes ages, longitude-latitude coordinates, lithology, and data sources. We use the original data documents to obtain the exact ages of the volcanic rocks and exclude samples without age data. Thus, we select 371 samples from the EarthChem rock database, then check the accuracy of the data and amend the erroneous data. To improve representation, we supplement the database by collecting further data on the Middle–Late Mesozoic volcanic rocks from the NCC with accurate ages. The data set is filtered using the following criteria: (a) only analyses published after 2,000 are considered; (b) ages obtained using methods with a relatively high precision ($^{40}Ar/^{39}Ar$ or zircon U-Pb) are compiled, while Rb-Sr, K-Ar, and fission track ages are excluded; (c) samples with the high loss on ignition (LOI > 4.0 wt. %) are also excluded. We use ferric oxide to characterize the iron content to solve the problem of different representations of iron oxides in the database and recalculate each oxide's percentage by subtracting LOI to obtain the exact proportions of each element and exclude the influence of volatiles. According to the above criteria, we extract 894 samples of the Middle–Late Mesozoic volcanic rocks from the NCC to discuss geochemical proxies such as major, trace elements, and isotopes. Finally, we use the corrected data to calculate the geochemical proxies such as P/Al and P/Yb ratios.

The 82 new samples investigated here are fresh volcanic rocks collected from the drill cores of Jurassic strata in Beipiao, Chaoyang (Figure 2d), and the stratigraphic sections of Yixian Formation from Xinkailing (41°36′50.39″ N, 120°47′15.65″ E) to Sihetun (41°35′26.20″ N, 120°47′49.44″ E) in Beipiao and from Mashenmiao (41°29′21.62″ N, 121°00′40.27″ E) to Songbahu (41°27′49.53″ N, 121°10′35.98″ E) in Yixian (Figure 2d). Examination of petrographic thin sections reveal that rock samples had not experienced significant alteration. Powder samples of the rocks are suitable for the whole-rock major and trace element analyses. The whole-rock major and trace element analyses are conducted at the Guangzhou ALS Laboratory, China.

3.2. Methods

This paper uses a central-moving resampling method to obtain the representative mean P content and other geochemical proxies of these volcanic rocks, such as the SiO_2 content and P/Al ratio. The width of the sample window and the step are 2 Ma and 1 Ma under most circumstances, respectively. First, we classify the Middle–Late Mesozoic volcanic rocks according to location and lithology (mafic, intermediate and felsic). Then we calculate the mean P content and other geochemical proxies of a certain lithology in a specific area required in this study using the bootstrap resampling algorithm in MATLAB with 10,000 iterations (Supporting Information S1). The results for the ages have an uncertainty of ±1 Ma. Only the middle 95% of data for the means and standard errors (SEs) are used to remove the abnormal extreme values. Based on the original description in the reports of regional geological surveys and literature, the proportion of each lithology of the volcanic rocks in this area is determined. Thus, we can calculate the mean P content and other geochemical proxies of all volcanic rocks in this location. For the regions lacking geological data, the bootstrap resampling method is carried out directly to calculate the means and SEs of P content and other geochemical proxies in the volcanic rocks. Finally, we estimate the means and SEs of P content and other geochemical proxies in the Mesozoic volcanic rocks at the interval based on these calculations.

In addition, we calculate the P content in the volcanic rocks from western Liaoning corresponding to SiO_2 content using the bootstrap resampling algorithm in MATLAB (Supporting Information S1). The width of the sample window and the step are set at two wt.% SiO_2. We execute 10,000 iterations for the bootstrap resampled subsets and obtain the mean and SE for each two wt.% SiO_2 by calculating the mean and SE of the 10,000 resampled subsets. The results are shown in a diagram of P versus SiO_2 contents (Figure S1a in Supporting Information S1).

4. Different Magma Sources of the Mesozoic Volcanic Rocks

The Middle–Late Jurassic volcanic rocks on the NCC are mainly felsic rocks (Figure S1 in Supporting Information S1) with low MgO, Cr, Co, and Ni (Figure S2 in Supporting Information S1), indicating a relatively minor contribution of mantle peridotite. The volcanic rocks (Haifanggou and Lanqi formations) in drill cores from the Jin–Yang (Jinlingsi–Yangshan) basin also show similar geochemical signatures (Figure S2 in Supporting Information S1). Previous studies suggested that the Jurassic volcanic rocks in western Liaoning had negative $\varepsilon_{Nd}(t)$ (Figure S3 in Supporting Information S1) and originated from the ancient lower crust (Yang & Li, 2008). In contrast, the anomalously high contents of MgO, Cr, Co, and Ni (Figure S2 in Supporting Information S1) and high $\varepsilon_{Nd}(t)$ of close to zero (Figure S3 in Supporting Information S1) in the volcanics of ca. 159 Ma indicate that the formation of the volcanic rocks is related to the upwelling of mantle-derived mafic melt. The subduction of the paleo-Pacific plate triggered the underplating by these mafic melt and ensuing massive magmatism at the surface (Ma et al., 2012, 2015). The underplating of mafic melt provided heat for the partial melting of the lower crust and could cause a low degree of crust-mantle material exchange in the above interval. Hence, the felsic volcanic rocks in the Middle–Late Jurassic were mainly derived from the partial melting of the ancient lower crust of the NCC under the background of the paleo-Pacific subduction.

The Early Cretaceous volcanic rocks on the NCC are mainly mafic rocks (Figure S1 in Supporting Information S1) with high MgO, Cr, Co, and Ni, as represented by the volcanic rocks in the Mashenmiao–Songbahu and Xinkailing–Sihetun sections of the Yixian Formation (Figure S4 in Supporting Information S1). Previous studies have shown that these lavas originated from the lithospheric mantle (Zhang & Zheng, 2003; Zheng et al., 2018). The subduction of the paleo-Pacific plate caused the large-scale thinning of the lithosphere (up to 80–120 km) and destruction of the eastern NCC, associated with massive mafic volcanism (Sun et al., 2021; Tang et al., 2021; Wu et al., 2019; Zhang et al., 2014; Zhu et al., 2011). During this period, the lithospheric mantle of the NCC became enriched due to the modification by subducted materials (Ma & Xu, 2021; Wu et al., 2019), as evidenced by the negative $\varepsilon_{Nd}(t)$ (Figure S3 in Supporting Information S1). Given the stability of apatite in subduction zones (Konzett & Frost, 2009), the efficient subduction of P into the mantle could result in a locally high-P mantle source for these Early Cretaceous volcanic rocks.

5. Regional Tectonics Determined the Variation of VPA

The VPA is variable with dominant lithology (Figure 2), and it is the function of the P contents of the volcanic rocks (Figure S5 in Supporting Information S1) and the intensity of volcanism (Supporting Information S1). The VPA of the samples from the drill cores and geological sections is mainly dependent on the P content of volcanic rocks (Supporting Information S1). These factors were severely affected by the deep Earth processes of the paleo-Pacific subduction and cratonic destruction during the Middle–Late Jurassic and Early Cretaceous (Zhu et al., 2011).

5.1. The Paleo-Pacific Subduction Affected the Intensity of Volcanism

As mentioned earlier, the Middle–Late Jurassic volcanic rocks in western Liaoning, northern NCC, resulted principally from the melting of the lower crust under the geodynamic setting of plate subduction. The magma source of the Early Cretaceous volcanic rocks was the lithospheric mantle modified by subduction-related melt/fluid. There are many factors affecting the intensity of volcanism, including the melting temperature and pressure and the composition of the magma sources. These factors are considerably controlled by the regional tectonic background of the cratonic destruction resulting from the paleo-Pacific subduction (Sun et al., 2021; Zhu et al., 2020). Hence, the paleo-Pacific subduction could ultimately affect the intensity of volcanism and thus VPA in the Middle–Late Jurassic and Early Cretaceous volcanic rocks in western Liaoning, northern NCC.

5.2. Effects of the Lithospheric Thickness on Volcanic P Content

Hahm et al. (2014) proposed that the chemical property of weathered bedrock, especially P content, exerts a first-order control on the biological colonization of habitats and the distribution of ecosystems. Hence, it is necessary to discuss the driving mechanism for the variation of P content in the volcanic rocks based on the geochemical behavior of phosphorus. A positive relationship between alkalinity and P content is existent in alkaline rocks (Green & Watson, 1982). However, the volcanic rocks of Haifanggou–Lanqi and Yixian formations show a negative correlation between alkali and P contents (Figure S6 in Supporting Information S1). In addition, there is no significant correlation between alkalinity and P content in the Middle–Late Jurassic and Early Cretaceous volcanic rocks, except for a few samples with enrichments of alkali and P (Figure S7 in Supporting Information S1). These facts imply that we cannot explore the cause of change in P content only from the perspective of alkalinity.

For the Middle–Late Jurassic volcanic rocks on the NCC, geochemical analysis shows that the variation trend of SiO_2 content with age is opposite to that of P and TiO_2 content (Figures 3a–3c), and the same is true for the Jurassic volcanic rocks in the Jin–Yang basin (Figures 3g–3i). This case is consistent with the negative correlation between SiO_2 and P content (Figure S1a in Supporting Information S1). These felsic volcanic rocks mainly originated from the partial melting of the lower crust, where lower content of SiO_2 and higher content of TiO_2 may be related to a relatively deep magma source (Niu, 2021; Xu, 2006), corresponding to the higher alkalinity of the rocks (Figures 3d and 3j).

The incompatibility of Ti is similar to that of Y (Gibson et al., 1996). However, Ti tended to enter the melts during partial melting when the depth of the magma source increased. The high Ti/Y ratios in the volcanic rocks at 166–164 Ma and 160–158 Ma (Figure 3e) resulted from the deepening of the magma source, consistent with the higher Ti/Y ratios in the volcanic rocks at the Haifanggou Formation and upper layer of Lanqi Formation (Figure 3k). Given that P behaves as an incompatible element in magmatic processes, the increased P content in the Jurassic volcanic rocks may result from crustal thickening. The secular variation of Sr/Y ratios that can reflect crustal thickness (Chapman et al., 2015; Profeta et al., 2015) suggests that the northern NCC experienced two significant crustal thickening processes between 169 and 158 Ma (Figure 3f). As shown in the secular variation of Sr/Y ratios (Figure 3l), the crust in western Liaoning thus could have experienced two significant crustal thickening events bounded by the lower layer of the Lanqi Formation.

Episode A of the Yanshanian Orogeny (Dong et al., 2008; Wong, 1927) included two compressional tectonic events, A1 (Early Callovian, ca. 168 Ma) and A2 (Middle Oxfordian, ca. 161 Ma) (Huang, 2019), which coincide well with the periods of significant increase of P content in the Jurassic volcanic rocks (Figure 3b). The compressional events increased the crustal thickness and decreased the melting degree, resulting in high P contents in the

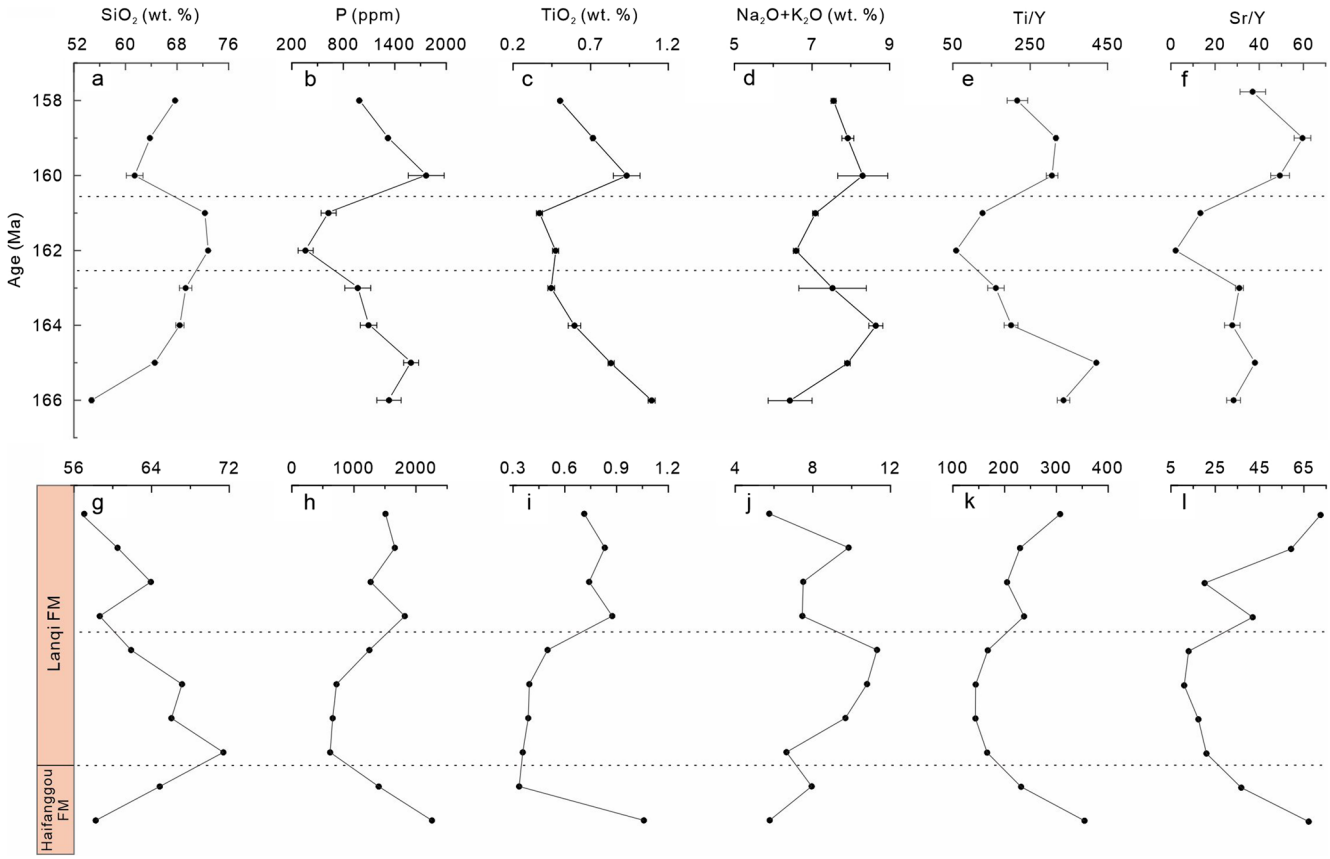

Figure 3. Temporal variations of geochemical proxies for the Middle–Late Jurassic volcanic rocks (166–158 Ma) on the North China craton (a–f) and the volcanic rocks of Haifanggou–Lanqi formations in the Jin–Yang basin (g–l). The Middle–Late Jurassic volcanic data are calculated from the compiled metadata (Section 3.2).

bottom (Haifanggou Formation) and top (upper Lanqi Formation) of the drill cores (Figure 3h). Since the change of subduction angle could lead to the transformation of the tectonic stress field, the two compressional events might result from the paleo-Pacific plate subduction (Huang, 2019; Zhu et al., 2020). The subducted materials were responsible for mantle melting and then mafic magma underplating. Hence, these deep-Earth processes changed the composition and intensity of volcanism, as manifested by the spatiotemporal distribution and secular P variation of volcanic rocks on the NCC. The observed changes in P content and scale of volcanic rocks and thus VPA are shown schematically in Figures 4a and 4b.

The solubility of P in mafic melts is higher than in felsic melts (Green & Watson, 1982; Watson, 1980; Watson & Capobianco, 1981), leading to the enrichment of P in mafic rocks. Thus the high P content in the Early Cretaceous volcanic rocks could result from their mafic compositions (Figures 5a and 5b), represented by the Yixian Formation volcanic rocks with low SiO_2 content (Figures 5i and 5q). The TiO_2 and alkali contents had almost no fluctuation between 126 Ma and 123 Ma (Figures 5c and 5d), indicating that the degree of partial melting did not change significantly. The higher contents of MgO, Cr, Co, and Ni (Figure S4 in Supporting Information S1) reflect the more contribution of the deeper mantle source. P contents gradually increased (Figures 5j and 5r) at volcanic cycle I of the Yixian Formation, whereas SiO_2 content decreased. There are no evident changes in TiO_2 content (Figures 5k and 5s) and alkalinity (Figures 5l and 5t) at the volcanic cycle I, suggesting that the degree of partial melting was almost unchanged. The SiO_2 content is lower, while MgO, Cr, Co, and Ni contents are higher in the volcanic rocks at the volcanic cycle I (Figure S4 in Supporting Information S1), reflecting less input from crustal melts. Hence, mafic magma at the volcanic cycle I had high P contents. These lines of evidence confirm the contribution of more mafic melts on the volcanic rocks with high P contents. The content of SiO_2 was higher (Figure 5a), while MgO, Cr, Co, and Ni contents were lower in the volcanic rocks before 128 Ma (Figure S4 in Supporting Information S1), reflecting more input of crustal melts at that time. However, the lack of this regularity in other periods suggested that other factors had a significant contribution, as evidenced by the radically

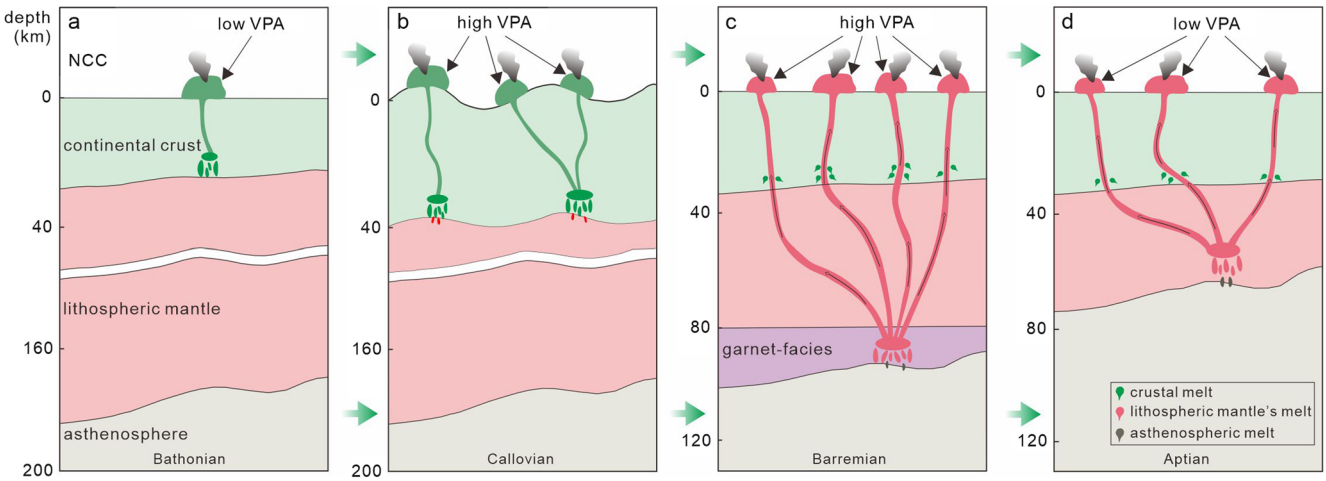

Figure 4. Simplified cartoon modified from Ma, Tang, Ye, et al. (2022), illustrating the origin of the Jurassic felsic volcanic rocks, the Cretaceous mafic volcanic rocks with different volcanic P availability (VPA). The occurrence and end of compression events in Episode A of the Yanshanian Orogeny changed the thickness of the crust and volcanic scale, and thus controlled the variation of VPA in the Haifanggou–Lanqi formations (a), (b). As the lithosphere thinned, the garnet facies decreased gradually, and the scale of volcanism increased, which increased the VPA of the Yixian Formation (c). When the garnet facies disappeared completely, the high degree of partial melting led to the low VPA of the Yixian Formation (d).

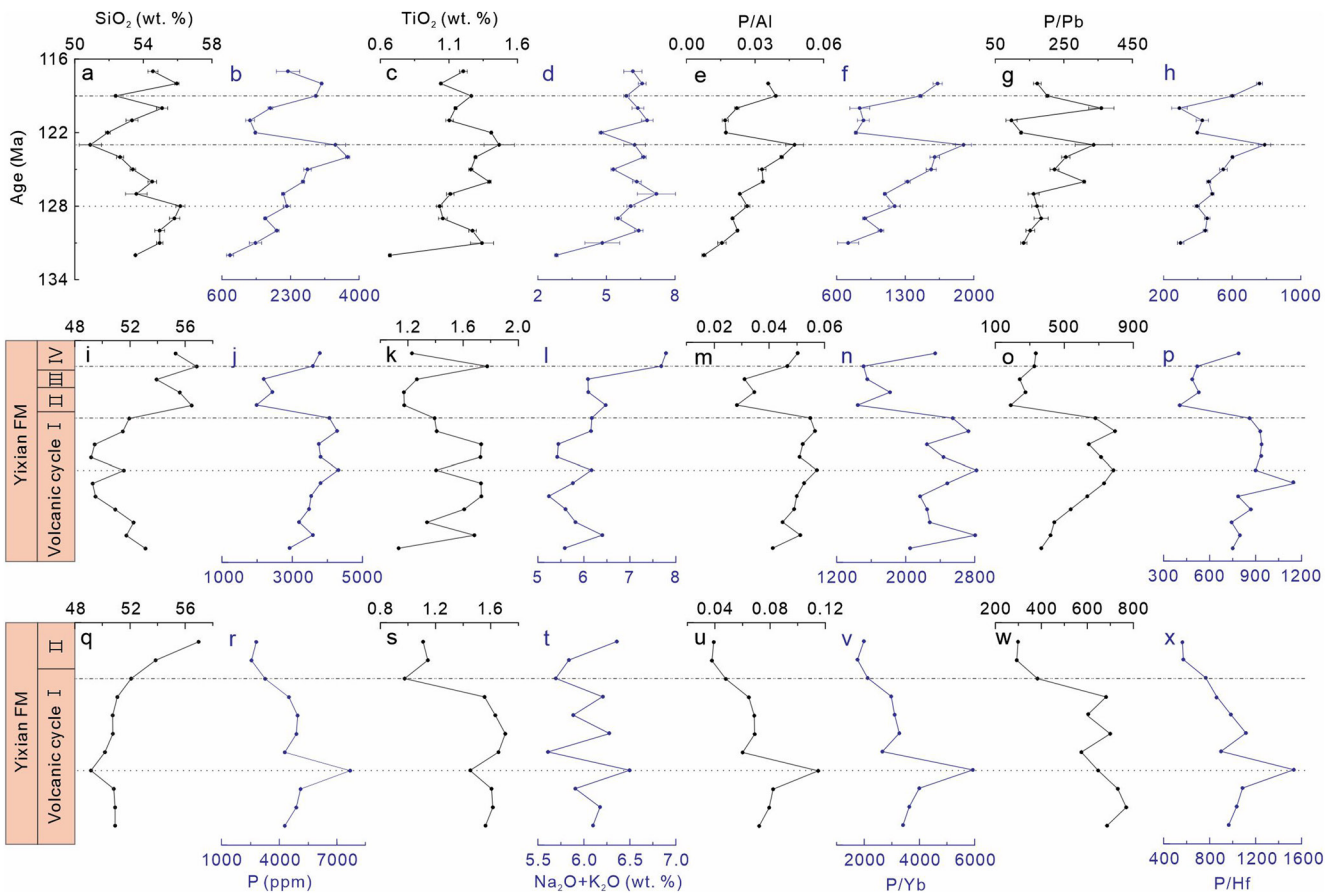

Figure 5. Temporal variations of geochemical proxies for the Early Cretaceous volcanic rocks (132–117 Ma) on the North China craton (a–h) and the volcanic rocks of the Yixian Formation in the Yixian (i–p) and Beipiao basins (q–x). Some P data of the Yixian volcanics are extracted from Ma, Tang, Ye, et al. (2022). The Early Cretaceous volcanic data are calculated from the compiled metadata (Section 3.2).

different P/Nd ratios before and after 123 Ma (Figure S8 in Supporting Information S1), even though P and Nd behave similarly in the magmatic processes (Sun & McDonough, 1989).

Ma, Tang, Ye, et al. (2022) considered that phosphate minerals are unlikely to be present on a large scale in magma source regions of these Early Cretaceous volcanic rocks, thus excluding the influence of apatite. The variation of P in mafic magmas likely implies the melt-garnet reaction and lithospheric thinning (Liu et al., 2016). Due to the structure of extreme preference for P (Konzett & Frost, 2009; Koritnig, 1965), garnet could contain more P than other mantle minerals, such as olivine and pyroxene (Haggerty et al., 1994; Konzett et al., 2011). Therefore, whether garnet is involved in the magmatism will significantly affect the P content in the mafic melts. The melt-rock reaction in the garnet stability field deeper than 80 km would inevitably reduce P content in ascending mafic melts. Thus, the variation of P content would be dependent on the length of melt-garnet reaction time controlled by the thickness of the garnet-facies lithospheric mantle.

Garnet is strongly rich in Yb and Al (Thompson, 1975). Thus, their geochemical behaviors are similar to P when garnet exists in the magma source region. In most cases, the P/Yb and P/Al ratios of the mafic volcanic rocks show similar trends. They changed sharply at 122 Ma (Figures 5e and 5f) and the boundary of the volcanic cycles I and II (Figures 5m-5n). These suggest that the influence of the melt-garnet reaction decreased along with the thinning of the lithosphere. The discontinuity at 122 Ma and the low value of P/Yb and P/Al ratios at the volcanic cycle II corresponded to the period when the garnet-facies mantle disappeared utterly.

The Pb and Hf prefer to enter the melts due to their incompatibilities. The P/Pb ratios show a similar increase pattern with P/Hf ratios before 123 Ma and a sharp drop at 122 Ma (Figures 5g and 5h). The abrupt changes of P/Pb and P/Hf ratios at 122 Ma correspond to the plunge in P content likely resulting from the destruction of garnet-facies lithospheric mantle. If caused by lithospheric thinning alone, the P/Pb ratio should be the highest, and the P/Hf be the lowest at 121 Ma. However, this was not observed because the outliers of these two ratios could reflect the significant addition of crustal melts consistent with a thin lithosphere in the period of 132–120 Ma, resulting in the substantial change of P content in the volcanic rocks. As for the volcanic rocks of the Yixian Formation, the P/Pb and P/Hf ratios increased in the cycle I (Figures 5o-5p, 5w-5x). Together with their abrupt drop in the cycle II, these facts suggest the P variation resulting from the disappearance of the garnet-facies mantle.

After the lithosphere was thinned to 120 km, the garnet-facies mantle gradually vanished, preventing the sequestration of P by garnet. The addition of P released from the garnet elevated the P content in the mafic melts before 123 Ma (Figure 5b). However, the partial melting degree in the magma source would be higher with the lithosphere becoming thinner than before, which would reduce the P content in melts. Combining these two factors resulted in the P content fluctuating at 132–120 Ma (Figure 5b). After 120 Ma, partial melting decreased with the lithospheric thickening due to mantle cooling, consistent with increased P content in the mafic volcanic rocks at 120–117 Ma and the stagnation period of magmatism at ca. 116–106 Ma (Xu, 2006). The mafic melts from different depths underwent different melt-peridotite reactions and crustal melt addition during their ascent processes, forming these Early Cretaceous volcanic rocks with different scales during the cratonic destruction. The observed changes in volcanic P content and scale and thus VPA are shown schematically in Figures 4c and 4d. Therefore, the changes in lithospheric thickness under the background of the paleo-Pacific plate subduction controlled the variation of VPA on the NCC during the Middle–Late Mesozoic.

6. Conclusions

Our study illustrates that the intensity of volcanism and composition variation of volcanic rocks were closely related to the cratonic destruction under the subduction system. The crustal thickening and subsequent lithospheric thinning triggered by the paleo-Pacific plate subduction caused the variation of volcanic P content and scale and thus volcanic P availability during the Middle–Late Mesozoic. These widespread Mesozoic volcanic rocks in western Liaoning, northern NCC, provided large amounts of available P for the terrestrial biosphere. The changes in VPA impacted the rise and fall of the Mesozoic terrestrial biotas. Consequently, the regional tectonics and corresponding deep processes could constrain the evolution of the terrestrial biotas through the volcanism and P cycle. The variation of P in volcanic rocks could provide crucial information on the coevolution of the deep-Earth processes and terrestrial biotas.

Data Availability Statement

The compiled and newly produced data for this paper are contained in the text, figures and supporting information and are also archived externally at https://doi.org/10.5281/zenodo.6837701.

Acknowledgments
We appreciate Rixiang Zhu and Jichang Zhu for providing core samples of the Jin–Yang basin, Wei Yang, Qiang Ma, Xinran Xu for the help with the field-work, and Min Wang for suggestions on the evolution of biotas. We thank the two anonymous reviewers for their thoughtful comments and the editor, Prof. Marie Edmonds, for her efficient handling. This work was supported by the National Natural Science Foundation of China (Grants 41725014 and 42288201).

References

Chang, S., Zhang, H., Renne, P. R., & Fang, Y. (2009). High-precision $^{40}Ar/^{39}Ar$ age constraints on the basal Lanqi Formation and its implications for the origin of angiosperm plants. *Earth and Planetary Science Letters*, *279*(3–4), 212–221. https://doi.org/10.1016/j.epsl.2008.12.045

Chapman, J. B., Ducea, M. N., DeCelles, P. G., & Profeta, L. (2015). Tracking changes in crustal thickness during orogenic evolution with Sr/Y: An example from the North American Cordillera. *Geology*, *43*(10), 919–922. https://doi.org/10.1130/g36996.1

Dilcher, D. (2000). Toward a new synthesis: Major evolutionary trends in the angiosperm fossil record. *Proceedings of the National Academy of Sciences of the United States of America*, *97*(13), 7030–7036. https://doi.org/10.1073/pnas.97.13.7030

Dong, S., Zhang, Y., Long, C., Yang, Z., Ji, Q., Wang, T., et al. (2008). Jurassic tectonic revolution in China and new interpretation of the "Yanshan Movement". *Acta Geologica Sinica - English Edition*, *82*(2), 334–347. https://doi.org/10.1111/j.1755-6724.2008.tb00583.x

Du, E., Terrer, C., Pellegrini, A. F. A., Ahlström, A., van Lissa, C. J., Zhao, X., et al. (2020). Global patterns of terrestrial nitrogen and phosphorus limitation. *Nature Geoscience*, *13*(3), 221–226. https://doi.org/10.1038/s41561-019-0530-4

Gibson, S. A., Thompson, R. N., Dickin, A. P., & Leonardos, O. H. (1996). Erratum to "High-Ti and low-Ti mafic potassic magmas: Key to plume—Lithosphere interactions and continental flood-basalt genesis". *Earth and Planetary Science Letters*, *141*(1), 325–341. [Earth Planet. Sci. Lett. 136 (1995) 149–165]. https://doi.org/10.1016/0012-821X(96)00041-6

Green, T. H., & Watson, E. B. (1982). Crystallization of apatite in natural magmas under high pressure, hydrous conditions, with particular reference to 'Orogenic'rock series. *Contributions to Mineralogy and Petrology*, *79*(1), 96–105. https://doi.org/10.1007/BF00376966

Haggerty, S. E., Fung, A. T., & Burt, D. M. (1994). Apatite, phosphorus and titanium in eclogitic garnet from the upper mantle. *Geophysical Research Letters*, *21*(16), 1699–1702. https://doi.org/10.1029/94GL01001

Hahm, W. J., Riebe, C. S., Lukens, C. E., & Araki, S. (2014). Bedrock composition regulates mountain ecosystems and landscape evolution. *Proceedings of the National Academy of Sciences of the United States of America*, *111*(9), 3338–3343. https://doi.org/10.1073/pnas.1315667111

Hartmann, J., Moosdorf, N., Lauerwald, R., Hinderer, M., & West, A. J. (2014). Global chemical weathering and associated P-release—The role of lithology, temperature and soil properties. *Chemical Geology*, *363*, 145–163. https://doi.org/10.1016/j.chemgeo.2013.10.025

Huang, D. (2019). Jurassic integrative stratigraphy and timescale of China. *Science China Earth Sciences*, *62*(1), 223–255. https://doi.org/10.1007/s11430-017-9268-7

Jiang, B., & Sha, J. (2006). Late mesozoic stratigraphy in Western Liaoning, China: A review. *Journal of Asian Earth Sciences*, *28*(4), 205–217. https://doi.org/10.1016/j.jseaes.2005.07.006

Kipp, M. A., & Stüeken, E. E. (2017). Biomass recycling and Earth's early phosphorus cycle. *Science Advances*, *3*(11), eaao4795. https://doi.org/10.1126/sciadv.aao4795

Konzett, J., & Frost, D. J. (2009). The high P–T stability of hydroxyl-apatite in natural and simplified MORB—An experimental study to 15 GPa with implications for transport and storage of phosphorus and halogens in subduction zones. *Journal of Petrology*, *50*(11), 2043–2062. https://doi.org/10.1093/petrology/egp068

Konzett, J., Rhede, D., & Frost, D. J. (2011). The high PT stability of apatite and Cl partitioning between apatite and hydrous potassic phases in peridotite: An experimental study to 19 GPa with implications for the transport of P, Cl and K in the upper mantle. *Contributions to Mineralogy and Petrology*, *163*(2), 277–296. https://doi.org/10.1007/s00410-011-0672-x

Koritnig, S. (1965). Geochemistry of phosphorus—I. The replacement of Si^{4+} by P^{5+} in rock-forming silicate minerals. *Geochimica et Cosmochimica Acta*, *29*(5), 361–371. https://doi.org/10.1016/0016-7037(65)90033-5

Lee, C. A., Jiang, H., Ronay, E., Minisini, D., Stiles, J., & Neal, M. (2018). Volcanic ash as a driver of enhanced organic carbon burial in the Cretaceous. *Scientific Reports*, *8*(1), 4197. https://doi.org/10.1038/s41598-018-22576-3

Liu, J., Chen, L., Zeng, G., Wang, X., Zhong, Y., & Yu, X. (2016). Lithospheric thickness controlled compositional variations in potassic basalts of Northeast China by melt-rock interactions. *Geophysical Research Letters*, *43*(6), 2582–2589. https://doi.org/10.1002/2016gl068332

Longman, J., Mills, B. J. W., Manners, H. R., Gernon, T. M., & Palmer, M. R. (2021). Late Ordovician climate change and extinctions driven by elevated volcanic nutrient supply. *Nature Geoscience*, *14*(12), 924–929. https://doi.org/10.1038/s41561-021-00855-5

Ma, C., Tang, Y., Ye, C., Ying, J., & Zhang, H. (2022). Mechanisms for phosphorus fluctuation in Phanerozoic volcanic rocks. *Lithos*, *424–425*, 106764. https://doi.org/10.1016/j.lithos.2022.106764

Ma, C., Tang, Y., & Ying, J. (2022). Volcanic phosphorus spikes associated with supercontinent assembly supported the evolution of land plants. *Earth-Science Reviews*, *232*, 104101. https://doi.org/10.1016/j.earscirev.2022.104101

Ma, Q., & Xu, Y. (2021). Magmatic perspective on subduction of Paleo-Pacific plate and initiation of big mantle wedge in East Asia. *Earth-Science Reviews*, *213*, 103473. https://doi.org/10.1016/j.earscirev.2020.103473

Ma, Q., Zheng, J., Griffin, W. L., Zhang, M., Tang, H., Su, Y., & Ping, X. (2012). Triassic "adakitic" rocks in an extensional setting (North China): Melts from the cratonic lower crust. *Lithos*, *149*, 159–173. https://doi.org/10.1016/j.lithos.2012.04.017

Ma, Q., Zheng, J., Xu, Y., Griffin, W. L., & Zhang, R.-S. (2015). Are continental "adakites" derived from thickened or foundered lower crust? *Earth and Planetary Science Letters*, *419*, 125–133. https://doi.org/10.1016/j.epsl.2015.02.036

McKenzie, N. R., Hughes, N. C., Gill, B. C., & Myrow, P. M. (2014). Plate tectonic influences on Neoproterozoic–early Paleozoic climate and animal evolution. *Geology*, *42*(2), 127–130. https://doi.org/10.1130/G34962.1

Niu, Y. (2021). Lithosphere thickness controls the extent of mantle melting, depth of melt extraction and basalt compositions in all tectonic settings on Earth—A review and new perspectives. *Earth-Science Reviews*, *217*, 103614. https://doi.org/10.1016/j.earscirev.2021.103614

Ott, R. F. (2020). How lithology impacts global topography, vegetation, and animal biodiversity: A global-scale analysis of mountainous regions. *Geophysical Research Letters*, *47*(20), e2020GL088649. https://doi.org/10.1029/2020GL088649

Pan, Y., Sha, J., Zhou, Z., & Fürsich, F. T. (2013). The Jehol Biota: Definition and distribution of exceptionally preserved relicts of a continental Early Cretaceous ecosystem. *Cretaceous Research*, *44*, 30–38. https://doi.org/10.1016/j.cretres.2013.03.007

Porder, S., & Ramachandran, S. (2012). The phosphorus concentration of common rocks—A potential driver of ecosystem P status. *Plant and Soil*, *367*(1–2), 41–55. https://doi.org/10.1007/s11104-012-1490-2

Profeta, L., Ducea, M. N., Chapman, J. B., Paterson, S. R., Gonzales, S. M., Kirsch, M., et al. (2015). Quantifying crustal thickness over time in magmatic arcs. *Scientific Reports*, *5*(1), 17786. https://doi.org/10.1038/srep17786

Reinhard, C. T., Planavsky, N. J., Gill, B. C., Ozaki, K., Robbins, L. J., Lyons, T. W., et al. (2017). Evolution of the global phosphorus cycle. *Nature*, *541*(7637), 386–389. https://doi.org/10.1038/nature20772

Rudnick, R. L., & Gao, S. (2014). Composition of the continental crust. In H. D. Holland & K. K. Turekian (Eds.), *Treatise on geochemistry* (2nd ed., pp. 1–51). Elsevier.

Ruttenberg, K. C. (2014). The global phosphorus cycle. In H. D. Holland & K. K. Turekian (Eds.), *Treatise on geochemistry* (2nd ed.), (Vol. 10, pp. 499–558). Elsevier.

Santosh, M. (2010). Supercontinent tectonics and biogeochemical cycle: A matter of 'life and death'. *Geoscience Frontiers*, *1*(1), 21–30. https://doi.org/10.1016/j.gsf.2010.07.001

Sun, P., Guo, P., & Niu, Y. (2021). Eastern China continental lithosphere thinning is a consequence of paleo-Pacific plate subduction: A review and new perspectives. *Earth-Science Reviews*, *218*, 103680. https://doi.org/10.1016/j.earscirev.2021.103680

Sun, S.-S., & McDonough, W. F. (1989). Chemical and isotopic systematics of oceanic basalts: Implications for mantle composition and processes. *Geological Society, London, Special Publications*, *42*(1), 313–345. https://doi.org/10.1144/gsl.Sp.1989.042.01.19

Tang, Y., Ying, J., Zhao, Y., & Xu, X. (2021). Nature and secular evolution of the lithospheric mantle beneath the North China Craton. *Science China Earth Sciences*, *64*(9), 1492–1503. https://doi.org/10.1007/s11430-020-9737-4

Thompson, R. N. (1975). Is upper-mantle phosphorus contained in sodic garnet? *Earth and Planetary Science Letters*, *26*(3), 417–424. https://doi.org/10.1016/0012-821X(75)90017-5

Wang, X., Gao, S., Liu, X., Yuan, H., Hu, Z., Zhang, H., & Wang, X. (2006). Geochemistry of high-Mg andesites from the early Cretaceous Yixian Formation, Western Liaoning: Implications for lower crustal delamination and Sr/Y variations. *Science in China - Series D: Earth Sciences*, *49*(9), 904–914. https://doi.org/10.1007/s11430-006-2016-7

Watson, E. B. (1980). Apatite and phosphorus in mantle source regions: An experimental study of apatite/melt equilibria at pressures to 25 kbar. *Earth and Planetary Science Letters*, *51*(2), 322–335. https://doi.org/10.1016/0012-821X(80)90214-9

Watson, E. B., & Capobianco, C. J. (1981). Phosphorus and the rare Earth elements in felsic magmas: An assessment of the role of apatite. *Geochimica et Cosmochimica Acta*, *45*(12), 2349–2358. https://doi.org/10.1016/0016-7037(81)90088-0

Wong, W. H. (1927). Crustal movements and igneous activities in Eastern China since mesozoic time. *Bulletin of the Geological Society of China*, *6*(1), 9–37. https://doi.org/10.1111/j.1755-6724.1927.mp6001002.x

Wu, F., Yang, J., Xu, Y., Wilde, S. A., & Walker, R. J. (2019). Destruction of the north China craton in the mesozoic. *Annual Review of Earth and Planetary Sciences*, *47*(1), 173–195. https://doi.org/10.1146/annurev-earth-053018-060342

Xu, X., Zhou, Z., Sullivan, C., Wang, Y., & Ren, D. (2016). An updated review of the Middle-Late Jurassic Yanliao Biota: Chronology, taphonomy, paleontology and paleoecology. *Acta Geologica Sinica - English Edition*, *90*(6), 2229–2243. https://doi.org/10.1111/1755-6724.13033

Xu, X., Zhou, Z., Wang, Y., & Wang, M. (2020). Study on the Jehol Biota: Recent advances and future prospects. *Science China Earth Sciences*, *63*(6), 757–773. https://doi.org/10.1007/s11430-019-9509-3

Xu, Y. (2006). Using basalt geochemistry to constrain Mesozoic-Cenozoic evolution of the lithosphere beneath North China Craton. *Earth Science Frontiers*, *13*(2), 93–104.

Yang, S., He, H., Jin, F., Zhang, F., Wu, Y., Yu, Z., et al. (2020). The appearance and duration of the Jehol Biota: Constraint from SIMS U-Pb zircon dating for the Huajiying Formation in northern China. *Proceedings of the National Academy of Sciences of the United States of America*, *117*(25), 14299–14305. https://doi.org/10.1073/pnas.1918272117

Yang, W., & Li, S. (2008). Geochronology and geochemistry of the mesozoic volcanic rocks in Western Liaoning: Implications for lithospheric thinning of the north China craton. *Lithos*, *102*(1–2), 88–117. https://doi.org/10.1016/j.lithos.2007.09.018

Zaffos, A., Finnegan, S., & Peters, S. E. (2017). Plate tectonic regulation of global marine animal diversity. *Proceedings of the National Academy of Sciences of the United States of America*, *114*(22), 5653–5658. https://doi.org/10.1073/pnas.1702297114

Zerkle, A. L. (2018). Biogeodynamics: Bridging the gap between surface and deep Earth processes. *Philosophical Transactions of the Royal Society A: Mathematical, Physical and Engineering Sciences*, *376*(2132), 20170401. https://doi.org/10.1098/rsta.2017.0401

Zerkle, A. L., & Mikhail, S. (2017). The geobiological nitrogen cycle: From microbes to the mantle. *Geobiology*, *15*(3), 343–352. https://doi.org/10.1111/gbi.12228

Zhang, H., & Zheng, J. (2003). Geochemical characteristics and petrogenesis of mesozoic basalts from the North China craton: A case study in Fuxin, Liaoning Province. *Chinese Science Bulletin*, *48*(9), 924–930. https://doi.org/10.1007/BF03325677

Zhang, L. (2013). Main geological background during the evolution of Jehol Biota from Western Liaoning. *Global Geology*, *32*(3), 447–462.

Zhang, S., Zhao, Y., Davis, G. A., Ye, H., & Wu, F. (2014). Temporal and spatial variations of Mesozoic magmatism and deformation in the North China Craton: Implications for lithospheric thinning and decratonization. *Earth-Science Reviews*, *131*, 49–87. https://doi.org/10.1016/j.earscirev.2013.12.004

Zheng, Y., Xu, Z., Zhao, Z., & Dai, L. (2018). Mesozoic mafic magmatism in North China: Implications for thinning and destruction of cratonic lithosphere. *Science China Earth Sciences*, *61*(4), 353–385. https://doi.org/10.1007/s11430-017-9160-3

Zhou, Z., Jin, F., & Wang, Y. (2010). Vertebrate assemblages from the middle-late Jurassic Yanliao Biota in Northeast China. *Earth Science Frontiers*, *17*(Special Issue), 252–254.

Zhou, Z., Meng, Q., Zhu, R., & Wang, M. (2021). Spatiotemporal evolution of the Jehol Biota: Responses to the north China craton destruction in the early cretaceous. *Proceedings of the National Academy of Sciences of the United States of America*, *118*(34), e210785918. https://doi.org/10.1073/pnas.2107859118

Zhou, Z., & Wang, Y. (2010). Vertebrate diversity of the Jehol Biota as compared with other lagerstätten. *Science China Earth Sciences*, *53*(12), 1894–1907. https://doi.org/10.1007/s11430-010-4094-9

Zhou, Z., & Wang, Y. (2017). Vertebrate assemblages of the Jurassic Yanliao Biota and the early cretaceous Jehol Biota: Comparisons and implications. *Palaeoworld*, *26*(2), 241–252. https://doi.org/10.1016/j.palwor.2017.01.002

Zhu, R., Chen, L., Wu, F., & Liu, J. (2011). Timing, scale and mechanism of the destruction of the North China Craton. *Science China Earth Sciences*, *54*(6), 789–797. https://doi.org/10.1007/s11430-011-4203-4

Zhu, R., Zhou, Z., & Meng, Q. (2020). Destruction of the North China Craton and its influence on surface geology and terrestrial biotas. *Chinese Science Bulletin*, *65*(27), 2955–2965. https://doi.org/10.1360/tb-2020-0219